Orbital fluctuation theory in iron-based superconductors: s_{++}-wave superconductivity, structure transition, and impurity-induced nematic order

Hiroshi KONTANI[1], Yoshio INOUE[1], Tetsuro SAITO[1], Youichi YAMAKAWA[1], and Seiichiro ONARI[2]
[1] *Department of Physics, Nagoya University and JST, TRIP, Furo-cho, Nagoya 464-8602, Japan.*
[2] *Department of Applied Physics, Nagoya University and JST, TRIP, Furo-cho, Nagoya 464-8602, Japan.*
(Dated: February 28, 2013)

The main features in iron-based superconductors would be (i) the orthorhombic transition accompanied by remarkable softening of shear modulus, (ii) high-T_c superconductivity close to the orthorhombic phase, and (iii) nematic transition in the tetragonal phase. In this paper, we present a unified explanation for them, based on the orbital fluctuation theory, considering both the e-ph and the Coulomb interaction. It is found that a small e-phonon coupling constant ($\lambda \sim 0.2$) is enough to produce large orbital (=charge quadrupole $O_{xz/yz}$) fluctuations, which causes the s-wave superconductivity without sign reversal (s_{++}-wave state). The derived orbital fluctuations also cause the instability toward the structure transition due to the bound state formation of two orbitons with opposite momenta, which is called the "two-orbiton process". Moreover, impurity-induced non-local orbital order with C_2-symmetry is obtained when the orbital fluctuations are strong. This "impurity-induced nematic state" explains the in-plane anisotropy of resistivity in detwinned samples. We stress that (i)-(iii) are reproducible only when orbital fluctuations with respect to O_{xz} and O_{yz} charge quadrupoles are the most divergent. This fact ensures the reliability of the present model Hamiltonian and calculation.

keywords: iron-based superconducotrs, orbital fluctuation, superconductivity, structure transition, shear modulus softening

I. INTRODUCTION

Iron-based high-T_c superconductors had been discovered by Kamiahara *et al.* in 2008[1], and the highest superconducting (SC) transition temperature T_c at present reaches 56K. The SC state occurs when the crystal structure is tetragonal, which is realized by chemical doping (or applying the pressure) on mother compounds, through the structure transition from orthorhombic to tetragonal. In the phase diagram, the SC phase is next to the non-SC and metallic orthorhombic phase, and the structure transition at $T = T_S$ is second-order in $Ba(Fe,Co)_2As_2$[2]. Very large softening of shear modulus C_S suggests the existence of strong orbital (quadrupole) fluctuations[3–5]. Moreover, the spin-density-wave (SDW) state with $\mathbf{Q} \approx (\pi, 0)$ occurs in the orthorhombic phase, that is, T_N is close to but always lower than T_S. These experimental facts suggest a close relation between the mechanism of superconductivity and structure/orbital/SDW transition.

Although the lattice deformation in the orthorhombic phase is very small ($(a-b)/(a+b) < 0.003$), in-plane resistivity shows sizable anisotropy in the orthorhombic phase. This fact means that the structure transition is driven by electron-electron (or electron-optical-phonon) interaction, not by the cooperative Jahn-Teller effect due to electron-acoustic-phonon interaction. Very interestingly, large in-plane anisotropy starts to occur in the tetragonal phase at T^*, which is about 10K$\sim$100K higher than T_S in detwinned $Ba(Fe,Co)_2As_2$[6]. The discovery of this "nematic electronic state" free from lattice deformation had attracted great attention. The nematic transition also occurs in the tetragonal phase of $BaFe_2(As_{1-x}P_x)_2$, confirmed by the in-plane anisotropy in the magnetization ($\chi_a \neq \chi_b$) using the torque measurement under magnetic field[7]. These experimental facts offer us great hints to understand the electronic states and the pairing mechanism in iron-based superconductors.

Now, we have to try to construct a theory that can explain abovementioned main characters in pnictides in a unified way, not restricted to the superconductivity. In the early stage of the study of iron-based superconductors, however, many theorists had concentrated on the study of pairing mechanism. Based on spin fluctuation theories, fully-gapped sign-reversing s-wave ($s_{\pm}$-wave) state had been predicted[8–12]. The origin of the spin fluctuations is the intra-orbital nesting and the Coulomb interaction. However, the robustness of T_c against randomness in iron pnictides indicates the absence of sign-reversal in the superconducting (SC) gap[13–16]. Later, orbital-fluctuation-mediated s-wave state without sign reversal (s_{++}-wave) had been proposed[17–19]. The orbital fluctuations mainly originate from the inter-orbital nesting and the electron-phonon (e-ph) interactions due to non-A_{1g} optical phonons.

One of the main merits of the orbital fluctuation scenario is the robustness of the s_{++}-wave state against impurities or randomness, consistently many experiments[14–16]. Moreover, orbital-fluctuation-mediated s_{++}-wave state scenario is consistent with the large SC gap on the z^2-orbital band in Ba122 systems[18], observed by bulk-sensitive laser ARPES measurement[20]. Note that the "resonance-like" hump structure in the neutron inelastic scattering[6] is frequently explained as the spin-resonance due to the sign reversal in the SC gap[21,22]. However, experimental hump structure is well reproduced in terms of the s_{++}-wave SC state, rather

than the $s_{\pm}$-wave SC state, by taking the suppression in the inelastic scattering $\gamma(\omega)$ for $|\omega| \leq 3\Delta$ in the SC state (dissipationless mechanism)[23,24].

In this paper, we present recent developments of the orbital fluctuation theory presented in Refs.[17–19,25,26]. We present a unified explanation for the the following main characters in iron-based superconductors: (i) orthorhombic transition accompanied by remarkable C_S softening[3–5], and (ii) emergence of high-T_c superconductivity strong against randomness next to the orthorhombic phase. We also discuss (iii) "nematic transition" in the tetragonal phase[6] in terms of the impurity-induced non-local orbital order. It is noteworthy that (i)-(iii) can be explained only when orbital fluctuations with respect to O_{xz} and O_{yz} charge quadrupoles are the most divergent. This fact assures the reliability of the present theory and model Hamiltonian.

II. ORBITAL FLUCTUATIONS AND s_{++}-WAVE SUPERCONDUCTIVITY

A. Antiferro-orbital fluctuations due to inter-orbital nesting

Here, we study the five-orbital tight-binding model introduced in Refs.[8,27], which reproduces the experimental multiband structure very well. We also include both the Coulomb interaction (U, U', and J) and the quadrupole-quadrupole interaction induced by optical phonons. In this paper, we introduce the xyz-coordinate, in which x- and y-axes are along Fe-Fe direction.

Because of the symmetry of As_4 tetrahedron, Fe-ion optical phonon induces the following quadrupole-quadrupole interaction:[18],

$$H_{\rm quad} = -g(\omega_l) \sum_i \sum_{\Gamma}^{xz,yz,xy} \hat{O}^i_{\Gamma} \hat{O}^i_{\Gamma} \tag{1}$$

where $\hat{O}_{\Gamma,i}$ is the quadrupole operator for channel Γ at site i introduced in (I). $g(\omega_l) = g(0) \cdot \omega_D^2/(\omega_l^2 + \omega_D^2)$ is the quadrupole coupling induced by the optical phonons, were $\omega_D = 200 \sim 300$K is the phonon frequency and $w_l = 2\pi T l$ is the boson Matsubara frequency. Note that $\hat{O}_{\mu\nu} \propto \hat{l}_\mu \hat{l}_\nu + \hat{l}_\nu \hat{l}_\mu$, where $\hat{l}$ is the angular momentum. Here, we set $\langle xz|\hat{O}_{yz}|xy\rangle = \langle yz|\hat{O}_{xy}|xz\rangle = \langle xy|\hat{O}_{xz}|yz\rangle = 1$ by multiplying a constant. Recently, we have found that Eq. (1) is also caused by the multiorbital Coulomb interaction, by including the multiorbiton exchange process[?] that is absent in the random-phase approximation (RPA) [S. Onari and H. Kontani, arXiv:1203.28741].

In iron pnictides, antiferro-quadrupole (AFQ) fluctuations with respect to $\Gamma = xz/yz$ are induced by the quadrupole interaction and the inter-orbital nesting. The quadrupole susceptibility is $\chi^Q_{\Gamma}(\mathbf{q},\tau) = \int_0^\beta d\tau e^{i\omega_l \tau} \langle T_\tau \hat{O}_{\Gamma}(\mathbf{q},\tau) \hat{O}_{\Gamma}(\mathbf{q},0)\rangle$.

When $g = 0$, five quadrupole susceptibilities $\chi^Q_{\Gamma}(\mathbf{q})$ ($\Gamma = xz, yz, xy, z^2, x^2-y^2$) induced by Coulomb interaction are small and almost comparable, with peaks at $\mathbf{q} = (\pi, 0)$ or $(0, 0)$. By introducing small quadrupole interaction g, quadrupole susceptibilities with $\Gamma = xz, yz, xy$ are largely enhanced. The most divergent susceptibilities are $\chi^Q_{xz}(\mathbf{q})$ at $\mathbf{q} = (\pi, 0)$ and $\chi^Q_{yz}(\mathbf{q})$ at $\mathbf{q} = (0, \pi)$: They are approximately expressed as

$$\chi^Q_{\Gamma}(q) = \frac{c\xi^2}{1 + \xi^2(\mathbf{Q}_\Gamma - \mathbf{q})^2 - i\omega/\omega_0} \tag{2}$$

for $\Gamma = xz$ and yz, where $\mathbf{Q}_{xz} = (\pi, 0)$ and $\mathbf{Q}_{xz} = (0, pi)$. In two-dimensional systems, orbital fluctuation parameters behave as[29]

$$\xi^2 = l(T - T_{\rm AFQ})^{-1}, \tag{3}$$

$$\omega_0 = l'(T - T_{\rm AFQ}) \tag{4}$$

The Weiss temperature $T_{\rm AFQ}$ becomes zero at orbital quantum-critical-point (QCP). In eq. (3), the unit of the length is $a_{\rm Fe-Fe}(\approx 3$Angstrom).

In later sections, we will explain that the development of $\chi^Q_{xz(yz)}(\mathbf{Q}_{xz(yz)})$ gives rise to not only the s_{++}-wave state, but also the structure transition as well as impurity-induced nematic transition in the tetragonal phase. Although superconductivity can be caused by other orbital fluctuations (such as $\Gamma = xy$, x^2-y^2, or z^2), both structure and nematic transitions are uniquely explained only when $\Gamma = xz$ and yz are the most divergent. Therefore, the present orbital fluctuation model is considered to be reliable.

B. Phase diagram for $s_{\pm}$- and s_{++}-wave states

Figure 1 (a) shows the phase diagram obtained by the RPA (mean-field approximation) for the electron filling $n = 6.1$, where $g(0)$ is the quadrupole interaction and U is the intra-orbital Coulomb interaction; we set the Hund's coupling term $J = U/10$ and the inter-orbital term $U' = U - 2J$. a_c (a_s) is the charge (spin) Stoner factor; $a_c = 1$ ($a_s = 1$) corresponds to the orbital (spin) ordered state. For $U = 1.3$eV, orbital order appears when $g(0) \approx 0.16$eV, meaning that about 50% of orbital fluctuations originate from the Coulomb interaction. By solving the SC gap equation, we obtain the s_{++}-wave state when the orbital fluctuations dominate the spin fluctuations[17].

In Fig. 1 (b), we show the U-g phase diagram obtained by the FLEX approximation. The dashed-dotted line represents the condition $\alpha_c = 0.98$ at $T = 0.015$, corresponding to $g = 0.25 \sim 0.3$. Therefore, substantial orbital fluctuations emerge for $\lambda = gN(0) \lesssim 0.2$ even if the self-energy correction is taken into account. On the other hand, $\alpha_s = 0.95$ (0.92) for $U = 1.8$ and $g = 0$ (0.3) in the FLEX approximation, although $U_{\rm cr} = 1.25$

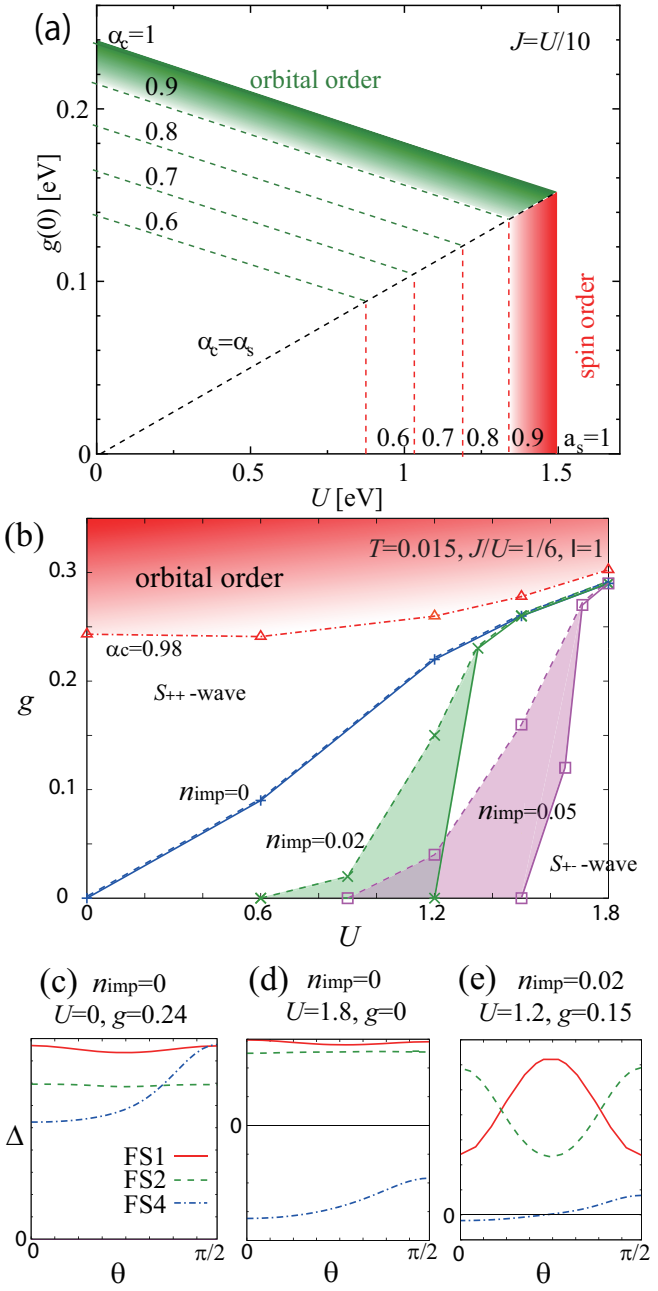

FIG. 1: g-U phase diagram obtained by (a) RPA for $J/U = 1/10$ and (b) FLEX approximation for $J/U = 1/6$. Also, (c)-(e) show the SC gap structure in FS1 (inner h-pocket), FS2 (outer h-pocket) and FS4 (e-pocket) for different model parameters. $\theta_{\mathbf{k}} = \tan^{-1}((k_y - k_y^0)/(k_x - k_x^0))$, where $\mathbf{k}^0$ is the center of each FS.

for $\alpha_s = 1$ in the RPA. Thus, the renormalization in α_s is rather larger than that in α_c. The region of the s_{++}-wave state is widely expanded in the presence of dilute impurities. In the present model, both $\chi^Q_{xz(yz)}$ and χ^Q_{xy} are strongly developed. Since all t_{2g}-orbitals on the Fermi surfaces are involved in these fluctuations, we obtained a fully-gapped s_{++}-wave state as shown in Fig. 1 (c), consistently with many high-T_c pnictides. When the spin fluctuations are comparable to orbital fluctuations, on the other hand, competition of these fluctuations induce the nodal structure in the SC gap, as shown in (e).

In summary, we discussed both the spin-fluctuation mediated $s_{\pm}$-wave state and orbital-fluctuation mediated s_{++}-wave state in iron-based superconductors. We have shown that the latter is realized by inter-orbital nesting in the presence of small quadrupole interaction g in eq. (1). Figure 1 (b) show the U-g phase diagram obtained by the FLEX approximation. Since both $s_{\pm}$- and s_{++}-states belong to the same A_{1g} symmetry, a smooth crossover from $s_{\pm}$-state to s_{++}-state is realized as increasing g or impurity concentration $n_{\rm imp}$. During the crossover, nodal s-wave state is realized, at which the obtained T_c is rather suppressed but finite. (Mathematically, it is impossible to distinguish between nodal s_{++}- and nodal $s_{\pm}$-states.) Experimentally, nodal line structure appears in $Ba(Fe_{1-x}Co_x)_2As_2$, in which both spin and orbital fluctuations are considered to be developed[30]. Recently, we have verified that the realization condition for the nodal structure is much moderate if we study a realistic "three dimensional" model[31].

C. heavily hole-doped system: KFe_2As_2

Here, we study the superconducting state in newly discovered heavily h-doped superconductor $K_xFe_2Se_2$ ($T_c \sim$ 30K) based on the ten-orbital model[25]. Since the hole-pockets are absent, the $s_{\pm}$-wave state is unlikely. However, when the Coulomb interaction is large enough, spin-fluctuation mediated d-wave state would appear due to the nesting between electron-pockets[32]. However, the symmetry of the body-centered tetragonal structure in $K_xFe_2Se_2$ requires the existence of nodes in the d-wave gap[25], although fully-gapped d-wave state is realized in the case of simple tetragonal structure. In the presence of moderate quadrupole interaction g, on the other hand, we find that orbital fluctuations give rise to the fully-gapped s_{++}-wave state.

In Fig. 2 (a), we show the α_c-dependence of the eigenvalue of the gap equation, $\lambda_{\rm E}$, for the s_{++}-wave state with $U = 0$, and the α_s-dependence of $\lambda_{\rm E}$ for the d-wave state with $g = 0$. In calculating the s_{++}-wave state, we use rather larger phonon energy; $\omega_D = 0.15$ eV, considering that the calculating temperature is about ten times larger than the real T_c. The SC gap functions for s_{++}-wave state are shown in Fig. 2 (b). The SC gap would become more anisotropic in case of $U > 0$.

Therefore, similar to iron-pnictide superconductors, orbital-fluctuation-mediated s_{++}-wave state is realized by small e-ph interaction $\lambda = gN(0) \sim 0.2$. The obtained $\lambda_{\rm E}$ for the s_{++}-wave state is larger than that for the spin-fluctuation-mediated d-wave state. We stress that nodal lines appear on the large e-pockets in the d-wave state, due to the hybridization between two e-pockets that is inherent in 122 systems, which is inconsistent with the

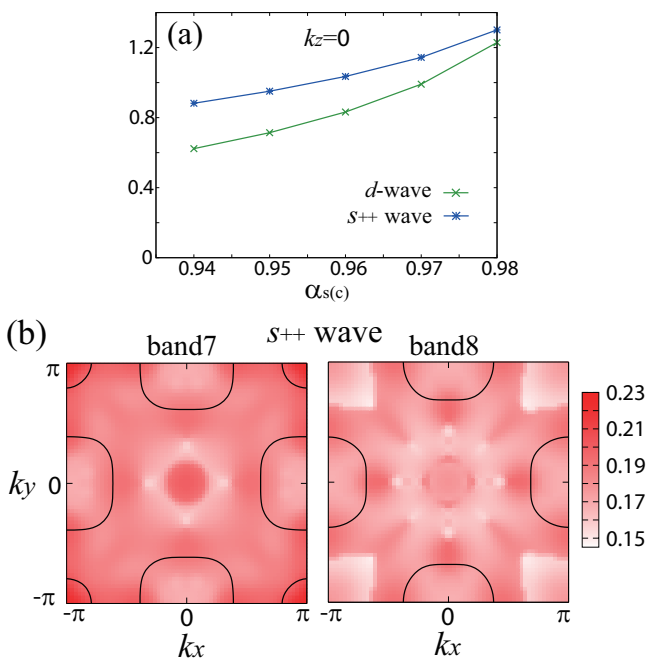

FIG. 2: (a) α_s- (α_c-) dependence of $\lambda_{\rm E}$ for d-wave (s_{++}-wave) state at $T = 0.03$ eV. (b) SC gap functions for s_{++}-wave state.

specific heat measurements[33] that report the isotropic SC gap. We propose that the study of impurity effect on $T_{\rm c}$ is useful since nodal d-wave state is fragile against impurities.

III. ORTHORHOMBIC STRUCTURE TRANSITION AND SOFTENING OF SHEAR MODULUS C_S

A. Two-orbiton mechanism

In many Fe-based superconductors, the SC state occurs next to the structure transition, suggesting a close relation between these two phenomena. Since the lattice deformation in the orthorhombic phase is very small ($(a-b)/(a+b) < 0.003$), we can safely rule out the cooperative Jahn-Teller effect due to electron-acoustic-phonon. Hereafter, we promise that $a = x$axis and $b = y$ axis. Below, we discuss the structure transition due to ferro quadrupole-quadrupole interaction.

For this purpose, we introduce the strain-quadrupole coupling:

$$H_S = \eta_S \sum_i \epsilon_S \hat{\phi}_S, \tag{5}$$

where ϵ_S is the strain for the orthorhombic deformation ($\epsilon_S \propto a-b$), $\hat{\phi}_S$ is a quadrupole operator that belong to the same representation of ϵ_S, and η_S is the coupling constant. Fernandes *et al.*[34] considered the "spin quadrupole operator" $\hat{\phi}_S = s_1 \cdot s_2$, where s_l represents the spin operator at sublattice $l = 1, 2$. (In their theory, stripe-type commensurate magnetic correlation is assumed.) In this case, $\hat{\phi}_S$ is a non-local operator. On the other hand, the present authors studied the "charge quadrupole operator" $\hat{\phi}_S = \hat{O}_{x^2-y^2}$, which is a local operator. In the presence of the strain-quadrupole coupling, the shear modulus C_S is given as

$$C_S^{-1} = C_{S,0}^{-1}(1 + g_S \chi_S(0,0)) \tag{6}$$

where $C_{S,0}$ is the lattice shear modulus, and $g_S = \eta_S^2 C_{S,0}^{-1}$. $\chi_S(\mathbf{q},\omega)$ is the total quadrupole susceptibility, given by the Fourier transformation of $\chi_S(\mathbf{q},\tau) \equiv \langle T_\tau \hat{\phi}_{\mathbf{q}}(\tau)\hat{\phi}_{-\mathbf{q}}(0)\rangle$.

Experimentally, C_S follows the Curie-Weiss relation in the under-doped systems with $T_S > 0$:

$$\frac{C_S}{C_{S,0}} = \frac{T - T_S}{T - \theta} \tag{7}$$

On the other hand, C_S deviates from the Curie-Weiss law in the over-doped systems without structure transition.

From now on, we consider the charge quadrupole susceptibility for $\hat{\phi} = \hat{O}_{x^2-y^2}$, $\chi^Q_{x^2-y^2}(0)$, based on the orbital fluctuation theory. In the RPA, the quadrupole interaction (1) together with the Coulomb interaction give rise to the AFQ fluctuations for the channels $\Gamma = xz, yz$ and xy, while $\chi^Q_{x^2-y^2}(0)$ remains small. Therefore, C_S softening cannot be explained within the RPA. However, the mode-mode coupling process with respect to $\chi^Q_{xz}(\mathbf{q})$ gives the development of ferro-quadrupole (FQ) fluctuations; $\chi^Q_{x^2-y^2}(0) \sim T\sum_{\mathbf{q}}\{\chi^Q_{xz}(\mathbf{q})\}^2$. This process is called the "two-orbiton term" in Ref.[26] since the condensation of composite bosons with zero momentum, $\hat{O}_{xz}(\mathbf{q})\hat{O}_{xz}(-\mathbf{q})$, induces the tetragonal structure transition, because of the relation $\hat{O}_{x^2-y^2} \propto \hat{O}^2_{xz} - \hat{O}^2_{yz}$. The two-orbiton term has close similarity to the Aslamazov-Larkin theory of excess conductivity given by superconducting fluctuations.

By taking the two-orbiton term, the irreducible susceptibility is given as

$$\chi^{\rm irr}_{x^2-y^2}(\mathbf{q}) = \chi^{(0)}_{x^2-y^2}(\mathbf{q}) + \chi_{\rm TO}(\mathbf{q}) \tag{8}$$

where $\chi^{(0)}_{x^2-y^2}(\mathbf{q})$ is the bare bubble term, and its temperature dependence is weak. Within the classical approximation, the two-orbiton term is $\chi_{\rm TO}(\mathbf{q}) = T\Lambda^2\sum_{\mathbf{k}}\chi^Q_{xz}(\mathbf{q}+\mathbf{k})\chi^Q_{xz}(\mathbf{k})$, where Λ is the three-point vertex[26]. The exact expression is given in eq. (61) in Ref.[26]:

$$\chi_{\rm TO}(0) = X\xi^2\left\{\frac{\omega_0}{\pi}\left[\psi\left(n_{\max} + \frac{\omega_0}{2\pi T} + 1\right) - \psi\left(\frac{\omega_0}{2\pi T} + 1\right)\right] + T\right\}, \tag{9}$$

where $\psi(x)$ is di-Gamma function, and $X \equiv \frac{(2g)^4 c^2}{4\pi}\Lambda^2$. ($c$ was introduced in eq. (2).) Since $\chi_{\rm TO}(\mathbf{q}) \propto T\xi^2$ for

$\mathbf{q} \to 0$, the two-orbiton term shows strong T-dependence. When $U = 0$, the total quadrupole susceptibility is given as

$$\chi^{Q}_{x^2-y^2}(\mathbf{q}) = \chi^{\rm irr}_{x^2-y^2}(\mathbf{q})/(1 - g_S \chi^{\rm irr}_{x^2-y^2}(\mathbf{q})) \qquad (10)$$

where g_S is the quadrupole-quadrupole interaction due to acoustic phonon. As a result, the elastic constant C_S is given by eqs. (6), (8) and (10), together with eq. (61) in Ref.[26].

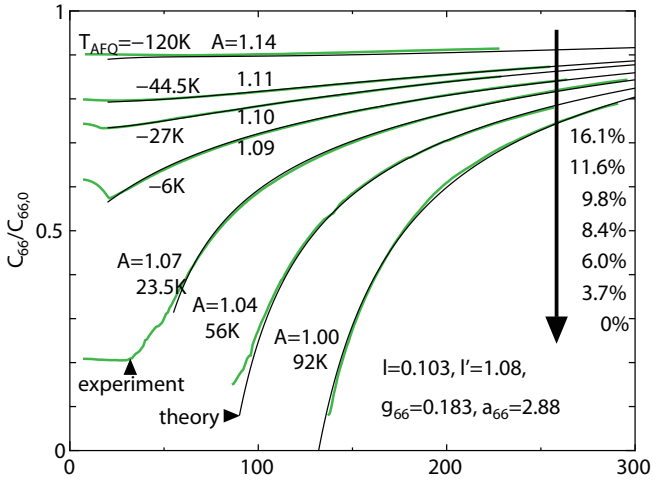

FIG. 3: $C_S/C_{S,0}$ given by the two-orbiton theory that reproduce experimental data for $Ba(Fe_{1-x}Co_x)_2As_2$ observed by Yoshizawa[4].

In Fig. 3, we plot $C_S/C_{S,0}$ based on the two-orbiton theory. We put orbital fluctuation parameters as $l = 1200$K, $l' = 1400$K, and $T_{\rm AFQ} = 92$K~ -120K. These values are consistent with theoretical calculation based on the FLEX approximation[19]. As for the spin fluctuation parameters in cuprates, $l = 0.2$eV (0.1eV) for $La_{1-x}Sr_xCuO_2$ ($YaBa_2Cu_3O_7$). We also set $g_S = 0.183$eV, $a_S \equiv \chi^{(0)}_{x^2-y^2}(0) = 2.88{\rm eV}^{-1}$, and $X \equiv \chi_{\rm TO}(0)/\xi^2 T = 5.47 \sim 7.11$.

In the FLEX approximation[19], $T_{\rm AFQ}$ changes from positive to negative by carrier doping, while other parameters (such as l and l') are insensitive to the doping. We can fit the recent experimental data by Yoshizawa *et al.*[4] for $Ba(Fe_{1-x}Co_x)_2As_2$ with $x = 0 \sim 16\%$, by changing $T_{\rm AFQ}$ from 90K to -120K, together with $X = 5.47 \to 7.11$. The fitting data shown in Fig. 3 reproduce the experimental data of Ref.[4] almost perfectly. This fact is a strong evidence for the success of orbital fluctuation theory in iron pnictide superconductors.

B. Phase diagram and SC transition temperature

We show the phase diagram for $Ba(Fe_xCo_{1-x})_2As_2$ in Fig. 4. T_c and T_S shows the experimental values, and $T_{\rm AFQ}$ is obtained by the fitting using the two-orbiton theory. While $T_{\rm AFQ}$ should almost coincide to T_S at $T_S = 0$ theoretically, the obtained $T_{\rm AFQ}$ slightly exceeds T_S for $x = 7 \sim 8\%$, because of the lack of experimental data at low temperatures. In fact, ξ^2 is expected to deviate from the Curie-Weiss behavior at low temperatures, as predicted by the SCR theory. In Fig. 4, θ is obtained experimentally by using the relation $(1 - C_S/C_{S,0})^{-1} \propto T - \theta$ when $C_S/C_{S,0}$ follows the Curie-Weiss relation in eq. (7).

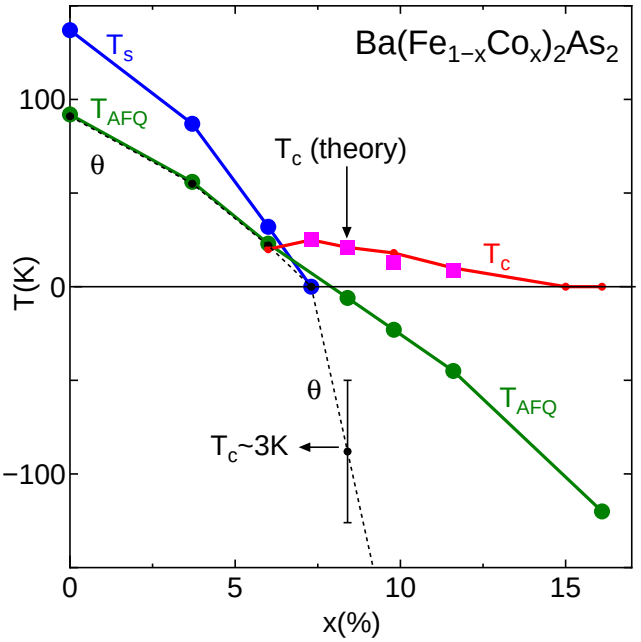

FIG. 4: Phase diagram for $Ba(Fe_xCo_{1-x})_2As_2$ obtained by the orbital fluctuation theory. $T_{\rm AFQ}$ is derived from the temperature dependence of C_S observed in Ref.[4]. We also show T_c derived from eq. (12) by solid squares using orbital fluctuation parameters derived from C_S

Based on the obtained orbital fluctuation parameters, we calculate the SC transition temperature. Here, we consider the orbital-fluctuation mediated s_{++}-wave state due to inter-pocket nesting. The linearized gap equation is given as

$$\lambda_E \Delta_\alpha(k, \epsilon_n) = \frac{\pi T}{(2\pi)^2} \sum_{\beta,p} \sum_m \int_\beta \frac{dp}{v^\beta_p} V_{\alpha,\beta}(k\epsilon_n, p\epsilon_m) \times \frac{\Delta_\beta(p, \epsilon_m)}{|\epsilon_m|} \qquad (11)$$

where λ_E is the eigenvalue; $\lambda_E = 1$ is satisfied at $T = T_c$. α, β represent Fermi surfaces (FSs), $k(p)$ is the momentum on the FS α (FS β), and $V_{\alpha,\beta}(k\epsilon_n, p\epsilon_m)$ is the interaction between (α, k) and (β, p). Here, we consider the attractive interaction due to orbital fluctuation; $V_{\alpha,\beta} \propto \chi^{Q}_{xz(yz)}$. For simplicity, we assume that both the Fermi velocity and SC gap are isotropic. Then, the momentum integration along the FS in eq. (11) can be performed as $\int_\beta \frac{dp}{v^\beta_p} V_{\alpha,\beta}(k\epsilon_n, p\epsilon_m) = C\xi/(1 + |\epsilon_n - \epsilon_m|/\omega_0)$,

where C is a constant. If we assume $\Delta_\alpha = \Delta_\beta$, we obtain the following simplified gap equation:

$$\lambda_E \Delta(\epsilon_n) = T \sum_\beta \sum_m \frac{C\xi - \mu^*}{1 + |\epsilon_n - \epsilon_m|/\omega_0} \frac{\Delta(\epsilon_m)}{|\epsilon_m|} \quad (12)$$

where μ^* is the Morel-Anderson pseudo potential; we put $\mu^* = 0.1$. We put $C = 0.075$ to obtain $T_c = 25$K when $T_{\rm AFQ} = 0$. In Fig. 4, we show the SC transition temperatures obtained by eq. (12) by solid squares, which are similar to experimental values. This fact means that the orbital fluctuation parameters derived from C_S are reasonable.

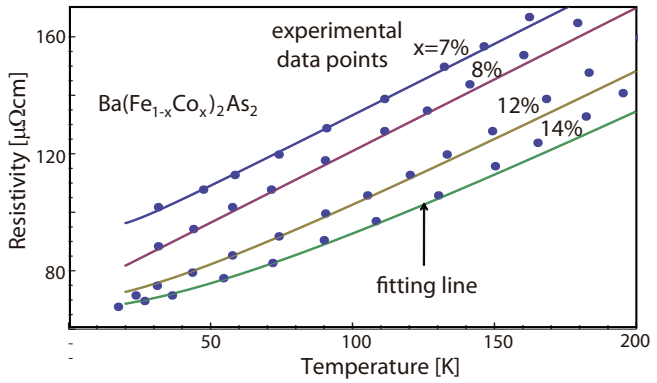

FIG. 5: Resistivity given by eq. (13), using the parameter $T_{\rm AFQ}$ derived from C_S. We can reproduce experimental data in $Ba(Fe_{1-x}Co_x)_2As_2$[35] below 200K very well.

Next, we discuss the non-Fermi-liquid behavior of the resistivity caused by the AF orbital fluctuations. In Fig. 5, circles show the resistivity of single crystal $Ba(Fe_{1-x}Co_x)_2As_2$ reported in Ref.[35]. According to spin/orbital fluctuation theory[29], the resistivity in two dimension is given as

$$\rho = AT^2\xi^2 + \rho_0 \quad (13)$$

where ξ is the correlation length of AF fluctuations, ρ_0 is the residual resistivity, and A is a constant. Using this equation together with $\xi^2 = l/(T - T_{\rm AFQ})$ derived from C_S, we can reproduce experimental data below 200K very well, as shown in Fig. 5. Here, we put $A = 0.49$ for all x, and $(T_{\rm AFQ}, \rho_0) = (-8, 80)$ for $x = 8\%$, $(0, 72)$ for $x = 10\%$, $(-50, 70)$ for $x = 12\%$, and $(-90, 67)$ for $x = 14\%$, respectively. ($T_{\rm AFQ}$'s are obtained from Fig. 4.) In the present theory, Fe-ion optical phonons together with the Coulomb interaction induce the AF-orbital fluctuations, which give rise to the s_{++}-wave state and non-Fermi-liquid-like transport phenomena. Moreover, two AF-orbitons with zero total momentum induce the ferro-orbital fluctuations, which are the origin of the orthorhombic structure transition. Therefore, the present orbital fluctuation theory can explain both the structure transition and the superconductivity.

C. Difficulties in other orbital fluctuation theories

Here, we discuss various difficulties in other orbital fluctuation models proposed for iron-based superconductors[36,37] To explain the orthorhombic structure transition, the ferro-$O_{x^2-y^2}$ fluctuations should be the most divergent. The $U' > U$ model in Ref.[36] cannot explain the structure transition since the most divergent fluctuation is O_{z^2}-type.

Next, we consider the "$O_{x^2-y^2}$-fluctuation model, in which all quadrupoles other than $O_{x^2-y^2}$ do not fluctuate. Then, electrons with xy-orbital character, which occupies one-third of the total DOS at Fermi level, are not involved in the $O_{x^2-y^2}$-fluctuations, since $\langle xy|\hat{O}_{x^2-y^2}|m\rangle = 0$ for any d-orbital m. This fact means that "gapless SC state with large residual DOS" is realized in the $O_{x^2-y^2}$-fluctuation model. Figure 6 shows the gap structure given by the (a) "$O_{xz/yz}$-fluctuation model" in Ref.[17] and (b) "$O_{x^2-y^2}$-fluctuation model" in Ref.[37]. In the latter model, the quadrupole interaction $H' = -g(\omega)\sum_i \hat{O}^i_{x^2-y^2} \cdot \hat{O}^i_{x^2-y^2}$ is introduced, considering the As-ion acoustic phonons. In (a), fully-gapped s_{++}-wave state is realized. In (b), in contrast, the SC gap on the xy-orbital hole-pocket around (π, π) in the unfolded BZ is almost gapless, and the SC gap on e-pockets is highly anisotropic. Therefore, $O_{x^2-y^2}$ fluctuation model cannot explain the fully-gapped nor nodal gap structure observed in almost all iron-based superconductors.

We also comment on the "T-linear resistivity" observed in various iron-based superconductors. In the ferro-$O_{x^2-y^2}$ fluctuation model, the portion of Fermi surfaces with xy orbital would become the cold-spot with $\gamma \propto T^2$. Thus, a conventional Fermi liquid behavior $\rho \propto T^2$ would be obtained in the ferro-$O_{x^2-y^2}$ fluctuation model, inconsistently with experiments.

Therefore, orbital fluctuations theories in Refs.[36,37] have serious difficulty in explaining the "fully-gapped" s_{++}-wave state as well as non-Fermi liquid transport phenomena in iron-based superconductors.

D. Effective Action

In Ref.[26], we have calculated the shear modulus C_S using the Green function method. Since the derivation was rather complex, we rederive the same expression in a more simple manner by introducing the Hubbard-Stratonovich field, in analogy to the analysis in Ref.[34]. By performing the Hubbard-Stratonovich transformation, we introduce the following effective action $S = S_0 + S_{\rm int} + S_{\rm strain}$ for the charge quadrupole field ϕ_Γ

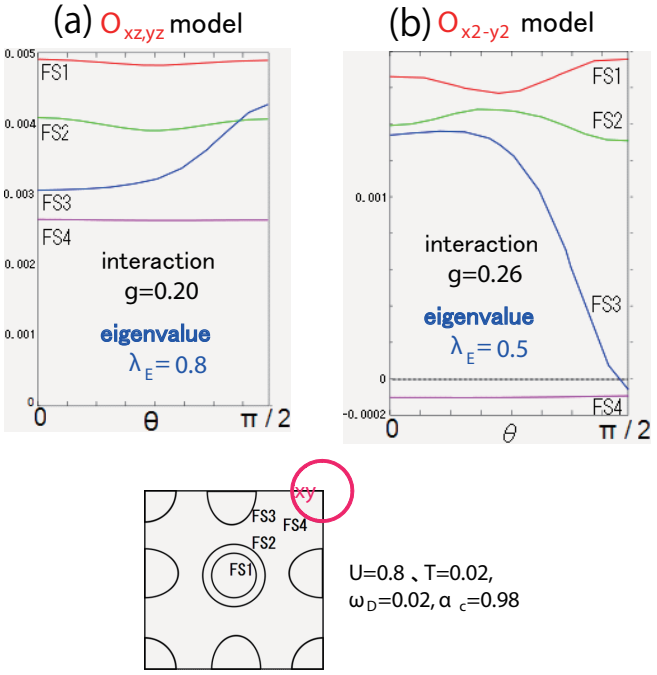

FIG. 6: The SC gap functions for $\alpha = 0.98$ in the (a) $O_{xz/yz}$-fluctuation model and (b) $O_{x^2-y^2}$-fluctuation model. In (b), the xy-orbital hole-pocket around (π, π) is almost gapless, since xy-orbital is not involved in the $O_{x^2-y^2}$-fluctuations. In (a), the eigenvalue of the gap equation (11), λ_E, is larger with smaller interaction g.

$(\Gamma = XZ, YZ)$:

$$S_0[\phi_\Gamma] = \frac{1}{2}\sum_{\Gamma}^{XZ,YZ}\int_q \left\{\chi^Q_\Gamma(q)\right\}^{-1}\phi^2_\Gamma(q), \quad (14)$$

$$S_{\rm int}[\phi_\Gamma] = -\frac{g'_S}{2}\int_x \{\phi_{XZ}(x)\phi_{YZ}(x)\}^2 \quad (15)$$

$$S_{\rm strain}[\phi_\Gamma] = \eta'_S\int_x \epsilon_S(x)\phi_{XZ}(x)\phi_{YZ}(x) \quad (16)$$

where $\int_x \cdots = \int_0^{1/T} d\tau \int d^2x \cdots$, S_0 represents the most divergent AF quadrupole susceptibility $\chi^Q_{XZ(YZ)}(q)$, $S_{\rm int}$ is the quadrupole-quadrupole interaction due to acoustic phonons, and $S_{\rm strain}$ is the strain-quadrupole coupling. In this subsection, we introduce the XY-coordinate that is -45 degree rotated from the xy-coordinate along z-axis. Apparently, $\phi_{XZ} = (\phi_{xz} - \phi_{yz})/\sqrt{2}$, $\phi_{YZ} = (\phi_{xz} + \phi_{yz})/\sqrt{2}$, and $O_{x^2-y^2} = O_{XY}$. In Eqs. (15) and (16), $g'_S \equiv g_S \cdot \Lambda^2$ and $\eta'_S \equiv \eta_S \cdot \Lambda$. where Λ is the three-point vertex with respect to (O_{XY}, O_{XZ}, O_{YZ}) that had been analyzed in Ref.[26].

Now, the quadrupole susceptibility $\chi^Q_{x^2-y^2}$ is given by the second derivative of the partition function with respect to $\eta\epsilon_S(x)$. If we put $g'_S = 0$, the quadrupole susceptibility is given as $\Lambda^2\chi^Q_{XZ}(x)\chi^Q_{YZ}(-x)$. By performing the Fourier transformation and taking the interaction g'_S into account, the total quadrupole susceptibility is obtained as

$$\chi^Q_{x^2-y^2}(q) = \Lambda^2\frac{\chi^{\rm irr'}(q)}{1 - g'_S\chi^{\rm irr'}(q)}, \quad (17)$$

$$\chi^{\rm irr'}(q) = \int_k \chi^Q_{XZ}(k+q)\chi^Q_{YZ}(q) + \Lambda^{-2}\chi^{(0)}_{x^2-y^2}(q) \quad (18)$$

where $\int_q \cdots = T\sum_n \int \frac{d^2q}{(2\pi)^2}\cdots$. Here, we have dropped both the vertex and self-energy corrections. Apart from the factor Λ^2, the first term the irreducible susceptibility (18) is equivalent to $\chi_{\rm TO}$ in eq. (9), or $\chi_{0,\rm nem}$ in Ref.[34]. We also added the bare susceptibility $\chi^{(0)}_{x^2-y^2}$ as the second term in eq. (18). Due to the two-orbiton term, $\chi^{\rm irr'}(0)$ is strongly enhanced near AFQ-QCP in proportion to ξ^2. When γ'_S is finite, $\chi^Q_{x^2-y^2}(0)$ diverges even if ξ is finite, and therefore the orthorhombic structure transition takes place in iron-based superconductors.

Note that the present action in eqs. (14)-(16) are mathematically equivalent to eqs. (3) and (4) in the spin-quadrupole theory in Ref.[34], by replacing ϕ_Γ $(\Gamma = XZ, YZ)$ with ϕ_i $(i = 1, 2)$, and $\chi^Q_\Gamma(q)$ with $\chi^s(q)$. Thus, the derived T-dependences of C_S are essentially the same. However, the coupling between strain and spin-quadrupole, η_S, would be too small to fit experimental data: We will discuss this issue below.

E. Comparison with spin quadrupole theory

As discussed in Sec. III, the orthorhombic structure transition is cause by the divergence of the FQ susceptibility with $\hat{x}^2 - \hat{y}^2$ symmetry. In this paper, we discussed the FQ fluctuation induced by the AF quadrupole fluctuations, due to the two-orbiton process. That is, antiferro-orbital fluctuations with respect to O_{XZ} and O_{YZ} (=orbitons) induce the s_{++} wave superconducting state, and the bound-state formation of two-orbitons with zero momentum, $O_{XZ}(\mathbf{q})O_{YZ}(-\mathbf{q}) \sim O_{XY}(0)$, give rise to the development of $\chi^Q_{XY}(0) = \chi^Q_{x^2-y^2}(0)$.

In this subsection, we discuss the "spin-nematic theory" for the structure transition discussed in Refs.[34,38], and explain a close relation to the two-orbiton mechanism. Their theories can be interpreted as the "two-magnon process" in our language. They had studied the non-local spin quadrupole operator $\hat{\phi}_S = m_1 \cdot m_2$ as explained in Sec. III A, and shown that the Ising-like order $\hat{\phi}_S \neq 0$ In both theories, the Ising-like order $(\langle\hat{\phi}_S\rangle \neq 0)$ occurs prior to the vector order $(\langle m_i\rangle, \langle(O_{xz}, O_{yz})\rangle \neq 0)$, since the latter is easily suppressed by thermal and quantum fluctuations. When the boson is orbiton (magnon), the realized superconductivity is the s_{++} $(\pm)$ wave state.

According to the fitting done in Sec. III, we have to assume $g_S \sim O(0.1)$eV to reproduce $E_{\rm JT} \equiv T_S - \theta \sim O(10)$K; the corresponding dimensionless e-ph coupling is

$\lambda \lesssim 0.1$. In this case, the required strain-quadrupole interaction η_S is about 0.5eV/Angstrom. As for the strain-charge-quadrupole interaction, $\eta_S^{\rm charge} \sim 0.5$eV is actually obtained by the point-charge model[17]. On the other hand, the strain-spin-quadrupole interaction $\eta_S^{\rm spin}$ would be of order $\sim \delta J(R)|m|^2/\delta R$, where $J(R)$ is the nearest-neighbor magnetic interaction and $|m|$ is the magnetic moment. Since $\delta J(R)/\delta R \sim 0.04$eV/Angstrom according to the first principle study[39], we expect that $\eta_S^{\rm spin}$ is one order of magnitude smaller than $\eta_S^{\rm charge}$. Then, there seems to be difficulty in reproducing the softening of C_S that occurs for a wide temperature range (from the room temperature to T_S; see Fig. 3) in terms of the spin-nematic scenario.

Finally, we note that the spin-quadrupole scenario requires that $\chi_s(\mathbf{q})$ is "commensurate". However, recent neutron experiment revealed that the magnetic order below T_N ($< T_S$) in $Ba(Fe_{1-x}Co_x)_2As_2$ is incommensurate for $x \geq 5.7\%$, although structure transition occurs for $x \geq 7\%$. This fact would support the realization of two-orbiton mechanism, since it does work even if $\chi^Q_{xz(yz)}(\mathbf{q})$ is incommensurate.

IV. IMPURITY-INDUCED NEMATIC ORDER

A. mean-field approximation

In previous sections, we have shown that both s_{++} wave superconductivity as well as the structure transition originate from the AF orbital fluctuations, $\chi^Q_{xz(yz)}(Q)$ caused by the inter-orbital nesting. In this section, we discuss the nematic ordered state in the tetragonal phase, which had been observed in many pnictides. For example, in $Ba(Fe_{1-x}Co_x)_2As_2$, large in-plane anisotropy starts to occur about 10∼100K higher than T_S[6]. This "nematic electronic state" free from lattice deformation had been also observed by ARPES measurements[20,40,41], optical conductivity measurements[42], and the anisotropy in the magnetic susceptibility[7]. The origin of this nematic order state had been one of the great open issues in iron-based superconductors.

Recently, local-density-of-states (LDOS) around impurity sites had been studied in detail by STM/STS technique, and nontrivial breakdown of the four-fold symmetry (C_{4v}) had been found in many pnictides. For example, single Co impurity induces a remarkable non-local change in the DOS along the a-axis (longer axis) with a length of $\sim 8a_{\rm Fe-Fe}$ in under-doped $Ba(Fe_{1-x}Co_x)_2As_2$[43]. Such a drastic impurity-induced anisotropic state is nontrivial since the orbital polarization in the orthorhombic phase is very small ($n_{xz} - n_{yz} \sim O(10^{-2})$). Similar impurity-induced non-local change in the DOS was also observed in LiFeAs with tetragonal structure by Hanaguri *et al*[44]. In many cases, impurity-induced states break the C_{4v}-symmetry, belonging to C_{2v}, C_2, or C_{1h}.

It would be natural to expect that impurity-induced low symmetric state explains the nematic phase above T_S. Recently, in-plane resistivity had been measured in detwinned $Ba(Fe_{1-x}Co_x)_2As_2$ crystals with high quality[45,46]. They found that $\rho_b - \rho_a$ is proportional to the Co concentration x for $x \leq 4\%$. Moreover, the residual resistivity per 1% Co impurity reaches $\sim 100\mu\Omega$cm, which exceeds the unitary limit of the local impurity potential ($\sim 20\mu\Omega$cm). Therefore, it had been proved experimentally that a Co impurity works as a strong scatter in the FeAs plane, like Zn impurity in cuprate superconductors.

In strongly correlated electron systems, impurity potential frequently causes nontrivial non-local change in the electronic state. For example, in nearly antiferromagnetic metals, antiferromagnetic correlation is drastically enhanced near the nonmagnetic impurity site, and the local magnetic moment emerges around the impurity. Such phenomena are indeed observed in under-doped cuprates[51]. As for the iron-based superconductors, the system would be close to antiferro-orbital QCP. Therefore, it is natural to expect the occurrence of "impurity-induced non-local orbital order" in pnictides.

In this section, we study the single impurity problem with potential I in ten-orbital tight-binding model for pnictides, using the mean-field approximation in real space Since we concentrate on the impurity-induced orbital-ordered state, we take only the quadrupole-quadrupole interaction in eq. (1) into account: We consider that the coupling constant g in eq. (1) originates from both the e-ph interaction as well as the multiorbital Coulomb interaction, as discussed in Sec. II. We obtain the following mean-field self-consistently for $g < g_c$, where $g_c = 0.221$ is the critical value for the bulk orbital order[47]:

$$M^i_{l,m} = \langle c^\dagger_{i,l\sigma} c_{i,m\sigma} \rangle_{I,g} - \langle c^\dagger_{i,l\sigma} c_{i,m\sigma} \rangle_{I,0} \tag{19}$$

where i is the Fe site, and l, m represent the d-orbital. Note that $M^i_{l,m}$ is impurity-induced mean-field for $g < g_c$ since it vanishes when $I = 0$. Then, the mean-field potential is given as

$$S^i_{l,m} = 2 \sum_{l',m'} \Gamma^c_{lm,l'm'} M^i_{l',m'} \tag{20}$$

and the mean-field Hamiltonian is $\hat{H}_{\rm MF} = \hat{H}_0 + \sum_i \hat{S}^i +$ const. Γ^c is the bare four-point vertex for the charge sector. We solve eqs. (19)-(20) self-consistently.

Since the present mean-field has 15 components at each site, it is convenient to consider the following quadrupole order:

$$O^i_\Gamma = 2 \sum_{l,m} o^{l,m}_\Gamma M^i_{l,m} \tag{21}$$

where $\Gamma = xz$, yz, xy, z^2, and $x^2 - y^2$. $o^{l,m}_\Gamma$ is the matrix element of the charge quadrupole operator given in Ref.[18]. We note that the hexadecapole ($l = 4$) order is negligible in the present study.

In Fig. 7, we show the obtained DOS in real space for the cluster of 800 Fe sites with a single impurity site[47]. First, we consider the case $I = -2$eV in (a)-(c). For $g = 0.200$ (a), the impurity induced mean-field is absent. The small modulation of the LDOS around the impurity is caused by the Friedel oscillation. For $g \geq 0.206$, impurity induced non-local orbital order is induced. The symmetry of the corresponding LDOS is C_{2v}, as shown in (b) for $g = 0.210$. The suppression of the DOS is caused by the non-local orbital order, consistently with a recent optical conductivity measurement[42]. The LDOS are further suppressed with increasing g, and the symmetry is lowered to C_2 for $g > 0.212$. In (c), we show the numerical result for $g = 0.216$ with C_2-symmetry. Similar impurity-induced LDOS with $C_{2(V)}$-symmetry is also obtained for a positive impurity potential. In contrast, we obtain the orbital order with C_4 symmetry for $I = +1$eV.

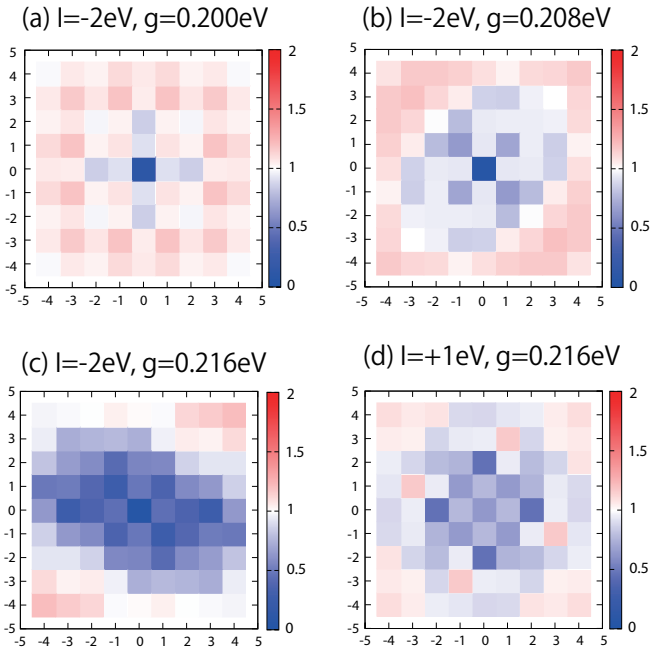

FIG. 7: Obtained LDOS given by the mean-field theory in the presence of impurity potential at $(0, 0)$. (a) $(I, g) = (-2, 0.200)$: without orbital order. (b) $(I, g) = (-2, 0.208)$: orbital order with C_{2v}-symmetry. (c) $(I, g) = (-2, 0.216)$: orbital order with C_2-symmetry. (d) $(I, g) = (+1, 0.216)$: orbital order with C_4-symmetry.

The dominant impurity-induced quadrupole orders are antiferro O_{xz}, O_{yz} and O_{xy}, reflecting the quadrupole-quadrupole interaction in eq. (1). The indispensable ingredient for C_2-order is the quadrupole interaction for $\Gamma = xz/yz$ channels. We have verified that the quadrupole interaction for $\Gamma = x^2 - y^2$ channel, which is caused by acoustic phonon, cannot realize the C_2-order.

By symmetry, the obtained C_2-order can be aligned by the strain-induced quadrupole potential, which is given in eq. (5) with $\hat{\phi}_S = O_{x^2-y^2}$. The effective quadrupole potential is $\Delta E = \eta_S \epsilon_S \cdot \chi^Q_{x^2-y^2}(0)/\chi^{(0)}_{x^2-y^2}(0)$, which is strongly enhanced near T_S due to the two-orbiton process as discussed in Sec. III A. This would be the reason why the nematic ordered state is easily detwinned by small uniaxial pressure near T_S. In fact, detwinning by uniaxial pressure is possible only when the structure transition is the second-order[48], in which case the factor $\chi^Q_{x^2-y^2}(0)/\chi^{(0)}_{x^2-y^2}(0)$ develops divergently. In over-doped systems, detwinning by pressure would be difficult since $\chi^Q_{x^2-y^2}(0)/\chi^{(0)}_{x^2-y^2}(0)$ is no more large[26].

B. in-plane anisotropy of resistivity

According to ARPES measurements in detwinned systems, $\Delta E < 0$ for $x = a$-axis is longer than $y = b$-axis, *i.e.*, $n_{xz} > n_{yz}$[40,41]. Then, experimentally observed $(\pi, 0)$ SDW order should be induced theoretically[26]. In this case, the C_2 order aligns along the $x = a$-axis in the present numerical results in Figs. 7 (c) and (d). We have calculated the in-plane resistivity ρ_a and ρ_b in the presence of dilute C_2 orders along a-axis using the T-matrix approximation, which gives the exact result when the impurity concentration is dilute and localization is negligible. We find that ρ_a is smaller than ρ_b by $\sim 40\%$, consistently with experimental reports. In Fig. 8 (a), we show the alignment of impurity-induced C_2 objects under uniaxial pressure. The anisotropy of resistivity in the nematic phase given by the T-matrix approximation is shown in Fig. 8 (b).

Here, we explain how to calculate the resistivity in the presence of aligned non-local orbital orders (nematic phase). The T-matrix is given by solving the following equation in the orbital-diagonal basis:

$$\hat{T}_{r,r'}(\omega) = (\hat{I} + \hat{S})_r \delta_{r,r'} + \sum_{r''} (\hat{I} + \hat{S})_r \hat{G}^{(0)}_{r-r''}(\omega) \hat{T}^{\mathrm{R}}_{r'',r'}(\omega) \quad (22)$$

where $\hat{S}$ is the mean-field potential, and $\hat{G}^{(0)}_r(\omega)$ is the Green function in real space without impurities. $\hat{I}_r = I\hat{1}\delta_{r,0}$ is the impurity potential. Note that $\hat{S}_r$ is diagonal with respect to the position since our interaction Hamiltonian is local.

The preset T-matrix is non-local because of $\hat{S}_r$ for $r \neq 0$. After the Fourier transformation, the self-energy due to multiple scattering in the T-matrix approximation is $\hat{\Sigma}(\mathbf{k}, \omega) = n_{\mathrm{imp}} T_{\mathbf{k},\mathbf{k}}(\omega)$, and the full Green function is $\hat{G}(\mathbf{k}, \omega) = (\omega + \mu - \hat{H}^0_{\mathbf{k}} - \hat{\Sigma}^{\mathrm{R}}(\mathbf{k}, \omega))^{-1}$. Then, the in-plane conductivity is given by

$$\sigma_\nu = \frac{e^2}{\pi} \sum_{\mathbf{k},\alpha} v^\alpha_{\mathbf{k},\nu} J^\alpha_{\mathbf{k},\nu} |G_\alpha(\mathbf{k}, i\delta)|^2 \quad (23)$$

where $\nu = x, y$, and α represents the αth band. $v_{\mathbf{k},\nu}$ is the group velocity of the αth band, and $G_\alpha(\mathbf{k}, \omega)$ is the full Green function in the band-diagonal basis. $J_{\mathbf{k},\nu}$ is

the total current including the current vertex correction, which is given by solving the following Bethe-Salpeter equation:

$$J^{\alpha}_{\mathbf{k},\nu} = v^{\alpha}_{\mathbf{k},\nu} + \sum_{\mathbf{p},\beta} I^{\alpha,\beta}_{\mathbf{k},\mathbf{p}} |G_{\beta}(\mathbf{p}, i\delta)|^2 J^{\beta}_{\mathbf{p},\nu} \tag{24}$$

where $I_{\mathbf{k},\mathbf{k}'} = n_{\rm imp}|T^{\rm R}_{\mathbf{k},\mathbf{k}'}(i\delta)|^2$ is the irreducible vertex. As shown in Fig. 8 (b), we obtain $\rho_b/\rho_a \sim 2$ in the nematic phase: The anisotropy is enhanced by including the current vertex correction.

Note that the averaged residual resistivity $(\rho_a + \rho_b)/2$ per 1% impurity with $I = +1$eV or -2eV reaches $\sim 50\mu\Omega$cm, which is comparable to the residual resistivity by 1% Co impurities in $Ba(Fe_{1-x}Co_x)_2As_2$; $50 \sim 100\mu\Omega$cm[14,46].

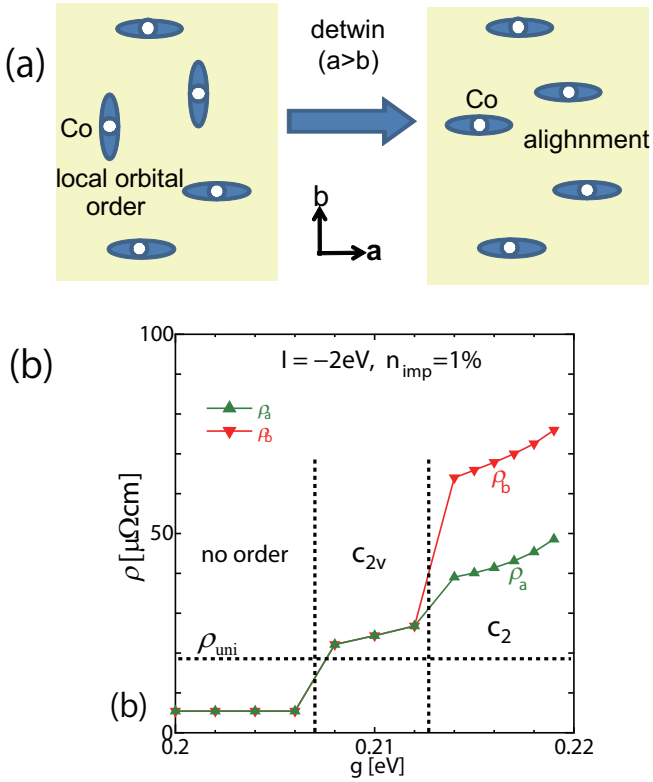

FIG. 8: (a) Detwinning of the impurity-induced C_2-orders under uniaxial pressure. The strain-induced effective quadrupole potential on each Fe is $\eta_S\epsilon_S(\chi^Q_{x^2-y^2}(0)/\chi^{(0)}_{x^2-y^2}(0))\hat{O}_{x^2-y^2}$. (b) In-plane anisotropy of resistivity in the nematic phase obtained by the T-matrix approximation. We assume 1% impurity with $I = -2$eV.

Here, we have studied the resistivity due to elastic scattering caused by spatially extended effective impurity potentials. In addition, strong antiferro fluctuations in pnictides should present various non-Fermi liquid transport phenomena in the normal state. In fact, relations $\rho \propto T$ and $R_{\rm H} \propto T^{-1}$ were observed in $BaFe_2(As,P)_2$[50]. Although such behaviors are frequently ascribed to the evidence of spin fluctuations[51], they are also brought by the development of antiferro-orbital fluctuations[19].

C. Comparison between theory and experiments

In a pure two-dimension system, a single nonlocal orbital order in the mean-field approximation might disappear by thermal and quantum fluctuations. In real systems, however, orbital order would be stabilized by the correlation between impurities for $n_{\rm imp} \gtrsim 1\%$. Since the AF fluctuations increase as T decreases in real systems, we can interpret that g monotonically increases as T decreases in the present mean-field approximation. Therefore, we expect that impurity-induced non-local orbital order is stabilized below the nematic transition temperature T^*, at which $g(T)$ would be close to g_c.

Although orbital order is absent above T^*, strong orbital fluctuations should appear near the impurity site, in analogy to the impurity-induced strong magnetic fluctuations realized in under-doped cuprates[49]. Therefore, inelastic scattering given by impurity-induced strong fluctuations causes large "residual resistivity" even above the impurity-induced Neel temperature[49]. By the same reason, residual resistivity in under-doped pnictides would be large even above T^*. The order parameters for the impurity induced nematic order are antiferro-$O_{xz/yz/xy}$, while the order parameter for the structure transition is ferro-$O_{x^2-y^2}$. Because of the difference in order parameters, T_S would be rather insensitive to the presence of impurities.

The nematic transition also occurs in the tetragonal phase of $BaFe_2(As_{1-x}P_x)_2$, which was confirmed by the in-plane anisotropy in the magnetization $(\chi_a \neq \chi_b)$ using the torque measurement under magnetic field[7]. In $BaFe_2(As_{1-x}P_x)_2$, P sites would works as impurities, which give finite potential on the neighboring for Fe sites. In this case, we had verified that non-local orbital order with C_2- or C_{1h}-symmetry appears around the impurity site in the mean-field approximation. In contrast, nematic order had not be observed in $(K,Ba)Fe_2As_2$[52], maybe because impurities outside of FeAs plane would be too weak to induce orbital order.

In this paper, we consider that the charge quadrupole order occurs at T_S, and the nematic order at T^* $(> T_S)$ originates from the impurity-induced orbital order. However, difference scenario had been proposed by the authors in Ref.[7]: They consider that the quadrupole order occurs at T^*, and T_S is just a meta-transition without symmetry breaking. In their phenomenological Landau model, very small orthorhombicity $(a-b)/(a+b)$ occurs below T^*, and it increases drastically below T_S as a meta-transition, consistently with experiments.

V. DISCUSSION

In the present paper, we have studied the realistic five-orbital model for iron pnictides. It was found that the O_{xz}-AFQ fluctuations develop owing to the quadrupole-quadrupole interaction due to e-ph and Coulomb interactions. This fluctuations not only cause the s_{++}-wave

superconductivity, but also the orthorhombic structure transition due to two-orbiton process. Using the two-orbiton term, we can fit the recent experimental data of C_S in $Ba(Fe_{1-x}Co_x)_2As_2$[4] for wide range of doping, only by choosing $T_{\rm AFQ}$ while other parameters are almost fixed. This fact is a strong evidence for the success of orbital fluctuation theory in iron pnictide superconductors.

However, we consider the impurity effect on the s_{++}-wave state: In the weakly correlated metals, impurity effect on the s_{++}-wave state is very small, known as the Anderson theorem. In strongly correlated metals, in contrast, impurity-induced change in the many-body electronic states could violate the Anderson theorem. In Sec. IV, we have shown that the impurity-induced orbital order causes remarkable reduction in the DOS, accompanied by the suppression of orbital fluctuations. For this reason, orbital-fluctuation-induced s_{++} wave state should be suppressed by impurities in the nematic state. In $Ba(Fe_{1-x}Co_x)_2As_2$, the suppression in $T_{\rm c}$ per 1% Zn-impurity, which gives a strong impurity potential, is $-\Delta T_c/\% \sim 3$K[16], while $-\Delta T_c/\% \sim 20$K is expected in the $s_{\pm}$-wave state when the mass-enhancement is $m^*/m_b \sim 3$[13]. Such small impurity-induced suppression of $T_{\rm c}$ in Ref.[16] would be naturally explained by the impurity-induced orbital order.

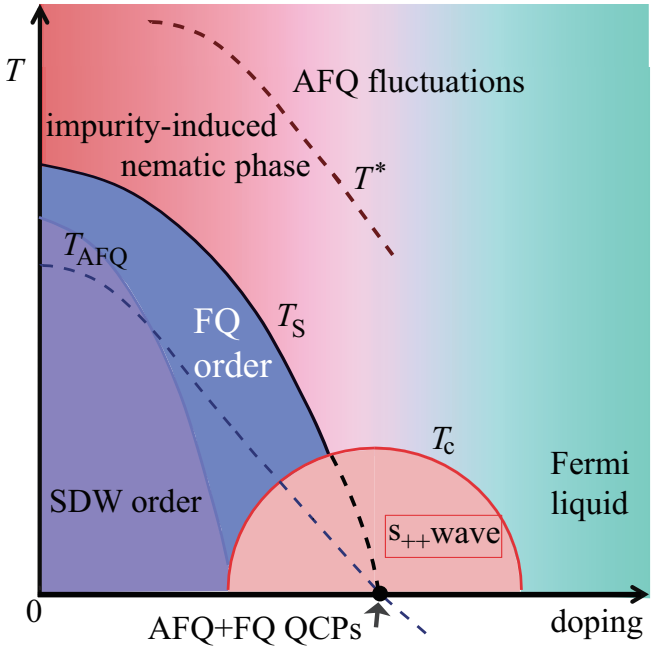

FIG. 9: The phase-diagram for iron-pnictide superconductors obtained by the present orbital fluctuation theory. T_S is the orthorhombic transition temperature (= FQ order temperature), and $T_{\rm N}$ is SDW transition temperature. The fact that two QCPs at $T_S = 0$ and $T_{\rm AFQ} = 0$ almost coincide means that novel "multi orbital QCPs" are realized in iron pnictides. At $T_{\rm AFQ}$, the AFQ-order does not occur since it is prevented by the FQ order at T_S. The impurity-induced nematic state is realized below T^*.

In Fig. 9, we summarize the phase-diagram of iron-pnictides given by the present orbital fluctuation theory. We stress that $T_{\rm AFQ}$, which is determined experimentally from C_S, is positive in the under-doped case ($T_S > 0$) while it is negative in the over-doped case. Especially, $T_S \approx 0$ for $T_{\rm AFQ} = 0$, consistently with experiments[4,5]. This result indicates that QCPs for AFQ and FQ orders almost coincide at the endpoint of the orthorhombic phase. Therefore, AFQ-QCP is not hidden inside of the orthorhombic phase, favorably to the orbital-fluctuation-mediated s_{++}-wave SC state[17–19]. Below T^*, impurity-induced orbital order with $C_{2(V)}$-symmetry starts to occur. Each orbital order can be aligned by applying tiny uniaxial pressure, resulting in the large in-plane anisotropy in the resistivity.

In summary, the present orbital fluctuation theory can explain the (i) superconductivity, (ii) orthorhombic transition accompanied by large softening of C_S, and (iii) impurity-induced nematic order. To explain (i)-(iii), we have to assume that $\chi^Q_{xz(yz)}$ is the most divergent quadrupole susceptibility, which is actually satified in the present model Hamiltonian. We have derived the orbital fluctuation parameters from C_S, and succeeded in explaining $T_{\rm c}$ and $\rho(T)$ using the derived parameters. These results are strong evidence for the realization of the orbital-fluctuation-mediated s_{++}-wave superconductivity in iron pnictides.

acknowledgements

We are grateful to D.S. Hirashima, D.J. Scalapino, P. Hirschfeld and A.V. Chubukov for valuable discussions on theories. We are also grateful to M. Sato, Y. Kobayashi, Y. Matsuda, T. Shibauchi, S. Shin, T. Shimojima and M. Yoshizawa for useful discussions on experiments. This study has been supported by Grants-in-Aid for Scientific Research from MEXT of Japan, and by JST, TRIP. Numerical calculations were performed using the facilities of the supercomputer center, Institute for Molecular Science.

[1] Y. Kamihara, T. Watanabe, M. Hirano, and H. Hosono: J. Am. Chem. Soc. **130**, 3296 (2008).
[2] C.R. Rotundu1 and R.J. Birgeneau: arXiv:1106.5761.
[3] M. Yoshizawa, R. Kamiya, R. Onodera, Y. Nakanishi, K. Kihou, H. Eisaki, and C. H. Lee, arXiv:1008.1479.
[4] M. Yoshizawa *et al.*, private communication.
[5] T. Goto, R. Kurihara, K. Araki, K. Mitsumoto, M. Akatsu, Y. Nemoto, S. Tatematsu, and M. Sato, J. Phys. Soc. Jpn. **80**, 073702 (2011); T. Goto *et al.* (unpublised)
[6] J.-H. Chu, J. G. Analytis, K. D. Greve, P. L. McMahon, Z. Islam, Y. Yamamoto, and I. R. Fisher, Science **329**, 824 (2010); J. J. Ying, X. F. Wang, T. Wu, Z. J. Xiang, R. H. Liu, Y. J. Yan, A. F. Wang, M. Zhang, G. J. Ye, P. Cheng, J. P. Hu, and X. H. Chen, arXiv:1012.2731; I.R. Fisher, L. Degiorgi, and Z.X. Shen, Rep. Prog. Phys. **74**, 124506 (2011).
[7] Y. Matsuda, private communication.
[8] K. Kuroki, S. Onari, R. Arita, H. Usui, Y. Tanaka, H. Kontani, and H. Aoki, Phys. Rev. Lett. **101**, 087004 (2008).
[9] I. I. Mazin, D. J. Singh, M. D. Johannes, and M. H. Du, Phys. Rev. Lett. **101**, 057003 (2008).
[10] S. Graser, G. R. Boyd, C. Cao, H.-P. Cheng, P. J. Hirschfeld, and D. J. Scalapino, Phys. Rev. B **77**, 180514(R) (2008).
[11] A. V. Chubukov, D. V. Efremov, and I. Eremin, Phys. Rev. B **78**, 134512 (2008).
[12] V. Cvetkovic and Z. Tesanovic, Europhysics Lett. **85**, 37002 (2009).
[13] S. Onari and H. Kontani, Phys. Rev. Lett. **103** 177001 (2009).
[14] A. Kawabata, S. C. Lee, T. Moyoshi, Y. Kobayashi, and M. Sato, J. Phys. Soc. Jpn. **77** (2008) Suppl. C 103704; M. Sato, Y. Kobayashi, S. C. Lee, H. Takahashi, E. Satomi, and Y. Miura, J. Phys. Soc. Jpn. **79** (2009) 014710; S. C. Lee, E. Satomi, Y. Kobayashi, and M. Sato, J. Phys. Soc. Jpn. **79** (2010) 023702.
[15] Y. Nakajima, T. Taen, Y. Tsuchiya, T. Tamegai, H. Kitamura, and T. Murakami, Phys. Rev. B **82**, 220504 (2010).
[16] J. Li, Y. Guo, S. Zhang, S. Yu, Y. Tsujimoto, H.Kontani, K. Yamaura, and E. Takayama-Muromachi: Phys. Rev. B **84**, 020513(R) (2011).
[17] H. Kontani and S. Onari, Phys. Rev. Lett. **104**, 157001 (2010).
[18] T. Saito, S. Onari, and H. Kontani, Phys. Rev. B **82**, 144510 (2010).
[19] S. Onari and H. Kontani, arXiv:1009.3882
[20] T. Shimojima, F. Sakaguchi, K. Ishizaka, Y. Ishida, T. Kiss, M. Okawa, T. Togashi, C.-T. Chen, S. Watanabe, M. Arita, K. Shimada, H. Namatame, M. Taniguchi, K. Ohgushi, S. Kasahara, T. Terashima, T. Shibauchi, Y. Matsuda, A. Chainani, and S. Shin, Sccience **332**, 564 (2011).
[21] T. A. Maier and D. J. Scalapino, Phys. Rev. B **78**, 020514(R) (2008); T. A. Maier, S. Graser, D.J. Scalapino, and P. Hirschfeld, Phys. Rev. B **79**, 224510 (2009).
[22] M. M. Korshunov and I. Eremin, Phys. Rev. B **78**, 140509(R) (2008).
[23] S. Onari, H. Kontani, and M. Sato, Phys. Rev. B **81**, 060504(R) (2010)
[24] S. Onari and H. Kontani, arXiv:1105.6233.
[25] T. Saito, S. Onari, and H. Kontani, Phys. Rev. B **83**, 140512(R) (2011).
[26] H. Kontani, T. Saito, and S. Onari, Phys. Rev. B **84**, 024528 (2011).
[27] T. Miyake, . Nakamura, R. Arita, M. Imada, J. Phys. Soc. Jpn. **79**, 044705 (2010)
[28] S. Onari and H. Kontani, unpublished.
[29] T. Moriya, *Spin Fluctuations in Itinerant Electron Magnetism* (Springer-Verlag, 1985); T. Moriya and K. Ueda, Adv. Physics **49** 555 (2000); T. Moriya and K. Ueda : Rep. Prog. Phys. **66** (2003) 1299.
[30] M. Yamashita, Y. Senshu, T. Shibauchi, S. Kasaharsa, K. Hashimoto, D. Watanabe, H. Ikeda, T. Terashima, I. Vekhter, A. B. Vorontsov, and Y. Matsuda Phys. Rev. B 84, 060507(R) (2011).
[31] T. Saito, S. Onari and H. Kontani, unpublished.
[32] T.A. Maier, S. Graser, P.J. Hirschfeld, and D.J. Scalapino, arXiv:1101.4988
[33] B. Zeng *et al.*, arXiv:1101.5117
[34] R.M. Fernandes, L. H. VanBebber, S. Bhattacharya, P. Chandra, V. Keppens, D. Mandrus, M.A. McGuire, B.C. Sales, A.S. Sefat, and J. Schmalian, Phys. Rev. Lett. **105**, 157003 (2010)
[35] F. Rullier-Albenque, D. Colson, A. Forget and H. Alloul, arXiv:0903.5243.
[36] Y. Yanagi, Y. Yamakawa and Y. Ono, Phys. Rev. B **81**, 054518 (2010).
[37] Y. Yanagi, Y. Yamakawa, N. Adachi and Y. Ono, J. Phys. Soc. Jpn. **79** (2010) 123707: They obtained fully-gapped SC gap since they introduced large $O_{xz/yz}$-type interaction in eq. (1 so that different fluctuations ($O_{x^2-y^2}$ and $O_{xz,yz}$) coexist. However, such coexistence is unexpected near the critical point.
[38] C. Fang, H. Yao, W.-F. Tsai, J. Hu, and S.A. Kivelson, Phys. Rev. B **77** 224509 (2008).
[39] T. Yildirim, Physica C **469** (2009) 425.
[40] Q. Wang, Z. Sun, E. Rotenberg, F. Ronning, E. D. Bauer, H. Lin, R. S. Markiewicz, M. Lindroos, B. Barbiellini, A. Bansil, D. S. Dessau, arXiv:1009.0271
[41] M. Yi, D. H. Lu, J.-H. Chu, J. G. Analytis, A. P. Sorini, A. F. Kemper, S.-K. Mo, R. G. Moore, M. Hashimoto, W. S. Lee, Z. Hussain, T. P. Devereaux, I. R. Fisher, Z.-X. Shen, PNAS **108**, 6878 (2011).
[42] L. Stojchevska, T. Mertelj, J.-H. Chu, Ian R. Fisher, and D. Mihailovic, arXiv:1107.5934.
[43] T.-M. Chuang, M.P. Allan, J. Lee, Y. Xie, N. Ni, S.L. Budko, G.S. Boebinger, P.C. Canfield and J.C. Davis, Science **327**, 181 (2010).
[44] T. Hanaguri, 26th International Conference on Low Temperature Physics, 2011.
[45] M. Nakajima, T. Liang, S. Ishida, Y. Tomioka, K. Kihou, C. H. Lee, A. Iyo, H. Eisaki, T. Kakeshita, T. Ito, and S. Uchida, PNAS **108**, 12238 (2011).
[46] S. Uchida, 26th International Conference on Low Temperature Physics, 2011.
[47] Y. Inoue, Y. Yamakawa and H. Kontani, arXiv:1110.2401.
[48] M.A. Tanatar, E.C. Blomberg, A. Kreyssig, M.G. Kim, N. Ni, A. Thaler, S.L. Budko, P.C. Canfield, A.I. Goldman, I.I. Mazin, and R. Prozorov, arXiv:1002.3801.
[49] H. Kontani and M. Ohno, Phys. Rev. B **74**, 014406 (2006).
[50] S. Kasahara, T. Shibauchi, K. Hashimoto, K. Ikada, S. Tonegawa, R. Okazaki, H. Shishido, H. Ikeda, H. Takeya, K. Hirata, T. Terashima, and Y. Matsuda, Phys. Rev. B

81, 184519 (2010).

[51] H. Kontani, Rep. Prog. Phys. **71**, 026501 (2008); H. Kontani and K. Yamada, J. Phy. Soc. Jpn. **74**, 155 (2005); H. Kontani, K. Kanki, and K. Ueda, Phys. Rev. B **59**, 14723 (1999).

[52] J. J. Ying, X. F. Wang, T. Wu, Z. J. Xiang, R. H. Liu, Y. J. Yan, A. F. Wang, M. Zhang, G. J. Ye, P. Cheng, J. P. Hu, and X. H. Chen, arXiv:1012.2731.